Distribution Agreement

In presenting this thesis as a partial fulfillment of the requirements for a degree from Emory University, I hereby grant to Emory University and its agents the non-exclusive license to archive, make accessible, and display my thesis in whole or in part in all forms of media, now or hereafter now, including display on the World Wide Web. I understand that I may select some access restrictions as part of the online submission of this thesis. I retain all ownership rights to the copyright of the thesis. I also retain the right to use in future works (such as articles or books) all or part of this thesis.

Ayla Khan March 28th, 2025

Identifying Antiviral Peptides to Inhibit HSV-1 Viral Replication

By

Ayla Khan

Elizabeth Bennett Draganova, PhD.
Advisor

Neuroscience & Behavioral Biology

Elizabeth Draganova, PhD.
Advisor

Leah Roesch, PhD.
Committee Member

Tyler Beyett, PhD.
Committee Member

2025

Identifying Antiviral Peptides to Inhibit HSV-1 Viral Replication

By

Ayla Khan

Elizabeth Bennett Draganova, PhD.
Advisor

An abstract of
a thesis submitted to the Faculty of Emory College of Arts and Sciences
of Emory University in partial fulfillment
of the requirements of the degree of
Bachelor of Sciences with Honors

Neuroscience & Behavioral Biology

2025

Abstract

Identifying Antiviral Peptides to Inhibit HSV-1 Viral Replication

By Ayla Khan

Herpes Simplex Virus-1 (HSV-1) is a neurotropic virus that establishes lifelong latency in the trigeminal ganglia, periodically reactivating to cause neuronal damage and symptomatic outbreaks. Currently, there is no cure or universal vaccine, and available antivirals are suboptimal. Therefore, we need novel prophylactic and therapeutic targets. One such target is herpesvirus nuclear egress, , an essential process in which the Nuclear Egress Complex (NEC), composed of UL31 and UL34, facilitates capsid transport across the nuclear envelope. The NEC oligomerizes on the nuclear membrane, binds to egressing capsids, and deforms the membrane to facilitate nuclear exit. Herein, we generated self-mimicking peptides intended to prevent NEC oligomerization, an essential aspect of NEC function. We screened the peptides for interactions with the NEC using biolayer interferometry and co-sedimentation assays. We identified one peptide that disrupted NEC heterodimer formation while others did not prevent the NEC from binding membranes, suggesting peptides likely perturb NEC oligomerization and not NEC/membrane associations. Future studies should explore peptide effects on NEC oligomerization, chemical crosslinking, optimize inhibitory design, and assess antiviral potential in neuronal models. Understanding how NEC-targeting peptides modulate HSV-1 replication may inform novel approaches to mitigating HSV-1-induced neurodegeneration and advancing antiviral strategies with potential applications for other neurotropic viruses.

Identifying Antiviral Peptides to Inhibit HSV-1 Viral Replication

By

Ayla Khan

Elizabeth Draganova
Advisor

A thesis submitted to the Faculty of Emory College of Arts and Sciences
of Emory University in partial fulfillment
of the requirements of the degree of
Bachelor of Sciences with Honors

Neuroscience & Behavioral Biology

2025

Acknowledgments

I would like to thank Dr. Elizabeth Draganova for allowing me the opportunity to work with her and her amazing lab, and for affording me the chance to learn and grow under her guidance. I would like to thank Rachel Hill, Neha Mohanty, and Maria Muhammad for their constant support and encouragement throughout my time in the lab. I would like to express my gratitude to Dr. Leah Roesch and Dr. Tyler Beyett for their support and for serving on my committee.

Table of Contents

Abstract

Herpes Simplex Virus-1 (HSV-1) is a neurotropic virus that establishes lifelong latency in the trigeminal ganglia, periodically reactivating to cause neuronal damage and symptomatic outbreaks. Currently, there is no cure or universal vaccine, and available antivirals are suboptimal. Therefore, we need novel prophylactic and therapeutic targets. One such target is herpesvirus nuclear egress, , an essential process in which the Nuclear Egress Complex (NEC), composed of UL31 and UL34, facilitates capsid transport across the nuclear envelope. The NEC oligomerizes on the nuclear membrane, binds to egressing capsids, and deforms the membrane to facilitate nuclear exit. Herein, we generated self-mimicking peptides intended to prevent NEC oligomerization, an essential aspect of NEC function. We screened the peptides for interactions with the NEC using biolayer interferometry and co-sedimentation assays. We identified one peptide that disrupted NEC heterodimer formation while others did not prevent the NEC from binding membranes, suggesting peptides likely perturb NEC oligomerization and not NEC/membrane associations. Future studies should explore peptide effects on NEC oligomerization, chemical crosslinking, optimize inhibitory design, and assess antiviral potential in neuronal models. Understanding how NEC-targeting peptides modulate HSV-1 replication may inform novel approaches to mitigating HSV-1-induced neurodegeneration and advancing antiviral strategies with potential applications for other neurotropic viruses.

Background and Introduction

Herpesviruses are double stranded DNA viruses capable of causing latent, lifelong infections in almost all mammals, including humans (Fatahzadeh & Schwartz, 2007). Herpesviruses can periodically reactivate and cause diseases that lead to high morbidity and mortality, particularly for the immunocompromised, for which there is no cure or universal vaccine (Johnston et al., 2014). Three subfamilies of herpesviruses infect humans: alpha-, beta-, and gamma herpesviruses. Herpes Simplex Virus Type 1 (HSV-1), from the alpha herpesvirus subfamily, is a neuroinvasive virus infecting approximately 70% of the human population, and is characterized by oral and genital sores, encephalitis, and keratitis (Boehmer et al., 2003).

After initial infection of epithelial cells (primarily in the skin or mucous membranes), HSV-1 spreads to the nervous system through retrograde transport via sensory neurons (Miranda-Saksena et al., 2018). Typically, HSV-1 establishes lifelong latency in the neurons of the peripheral nervous system, particularly the sensory ganglia, with the trigeminal ganglion being the most common reservoir (Otth, 2016). HSV-1 evades the host immune system, remaining dormant until reactivation is triggered by factors such as stress or immunosuppression (Whitley & Roizman, 2001). Upon reactivation, the virus travels back along the axons to the original infection site, where it can cause recurrent sores and in severe cases, conditions like herpes encephalitis or herpes keratitis (Bradshaw & Venkatesan, 2016).

The neuroinvasive and latent nature of HSV-1 has profound implications in both clinical and research contexts. HSV-1 infection of the central nervous system can result in herpes simplex encephalitis (HSE), which leads to significant morbidity and mortality, particularly when untreated in children (Johnston et al., 2014). HSE is the most common cause of viral encephalitis in the U.S., and despite treatment with antiviral therapies such as acyclovir, the neurovirulence of HSV-1 presents long-term neurological deficits in survivors. HSV-1 has also

been implicated in other neurodegenerative diseases, such as Alzheimer's, which further emphasizes its relevance in the study of neurobiology and neuropathology (Itzhaki, 2018).

During lytic infection, the process creating new viral particles, the assembly of new virions begins in the host cell nucleus. Here, the viral DNA is replicated, and new viral proteins are produced upon transcription and translation, allowing the formation of capsids filled with DNA. Once assembled, capsids can only become mature virions in the cytoplasm– yet the large size of capsids precludes nuclear pore export. Due to this inconvenience, capsids instead bud out of the nucleus at the inner nuclear membrane (INM), forming enveloped vesicles in the perinuclear space. Once formed, these vesicles then fuse with the outer nuclear membrane to be released into the cytoplasm (Roller & Baines, 2017). This unique biological process is called nuclear egress (Figure 1).

Nuclear egress is a vital step in the replication cycle of herpesviruses and is mediated by the viral nuclear egress complex (NEC), a virally encoded protein heterodimer essential for viral replication. The NEC is formed from two conserved viral proteins, UL31 and UL34 (Roller & Baines, 2017). UL34 is a 274-aa protein containing a single-spanning C-terminal transmembrane region (TM) that anchors the complex to the INM such that the NEC faces the nucleoplasm. In the absence of either protein, capsids accumulate in the nucleus, and viral titer is reduced at least 10,000-fold, suggesting both proteins are required for nucleus egress (Fuchs et al., 2002). Further, NEC expressed in uninfected cells produces empty perinuclear vesicles, indicating UL31 and UL34 are the only viral proteins required for nuclear budding to occur (Klupp et al., 2007). These findings maintain the NEC as a pivotal player in the process of nuclear budding and egress.

High-resolution structural studies showed that on membranes, the NEC assembles into a hexameric lattice that is essential for membrane budding deformation (Bigalke & Heldwein,

2016; Arii, 2021; Roller et al., 2010). The NEC lattice has two types of interfaces: hexameric (within hexamers) and interhexameric (between hexamers). Mutations designed to disrupt the lattice have been found to reduce budding *in vitro* and *in vivo* (Bjerke et al., 2003, Bigalke et al., 2014, Roller et al., 2010 and Draganova et al., 2024). In particular, these lattice mutations weaken hexameric lattice assembly and are incapable of budding, demonstrating how NEC activity can be inhibited by perturbing NEC oligomerization. Furthermore, NEC from various herpesviruses, including HSV-1, can be inhibited by peptides (Draganova et al., 2021) and small molecules (Chen et al., 2023), highlighting the ability of this protein to be inhibited.

This study aims to identify NEC sequence-specific peptides that can act as antiviral agents by inhibiting the budding process of the NEC, particularly by preventing NEC lattice assembly. Preliminary data using biolayer interferometry (BLI) identified peptides that bind to the NEC, but their inhibitory potential is still unknown. Specifically, the study aims to combine various *in vitro* assays to identify the mode of NEC inhibition, which could be occurring in two different ways: 1) peptides could prevent the NEC from binding to membranes, or 2) peptides could prevent NEC oligomerization by disrupting lattice formation. In both cases, budding levels would be reduced. To delineate these mechanisms, we utilized a well-established co-sedimentation assay (Thorsen et al., 2021) to determine if peptides preclude NEC/membrane interactions by using model membranes called multilamellar vesicles (MLVs).

I hypothesized that the presence of certain peptides will either inhibit the NEC's ability to induce membrane vesiculation by destabilizing NEC/membrane interactions or NEC heterodimer formation. These findings will help identify potential candidates for cellular delivery and evaluation of antiviral efficacy against HSV-1 in infected cells. Further, any antiviral peptides identified could open doors for new therapeutic strategies aimed at preventing the virus from invading the nervous system and protecting neuronal cells from HSV-1-induced damage.

Methodology

Peptide Screening Using Biolayer Interferometry (BLI)

A series of 15-aa peptides from the UL31 or UL34 amino acid sequences that correspond to either hexameric or interhexameric interfaces (described above) were purchased (Table 1). We conducted a high-throughput screen using BLI to identify binding interactions between the peptides and the NEC (either the truncated NECΔ40-190 or NEC220 constructs). BLI is a fiber optics method that reads changes in refractive index within individual biosensors. For our purposes, we utilized streptavidin-coated sensors that bind to biotinylated peptides. NEC, in a series of concentrations from 0 – 10 uM, was then introduced to the biosensors, and changes in the optical density of the sensor after the addition of the NEC typically reflected a binding event between the NEC and the peptide. Due to non-specific binding, K_D values were not determined and rather, the BLI was used as a binary screening tool for NEC interactions. From this screening, five distinct peptides were identified as possessing some binding character with the NEC (Table 2), and subsequent potential NEC inhibitory ability.

Multilamellar Vesicles (MLVs) Preparation

Following BLI peptide screening, we used an SDS-PAGE-based pelleting assay to monitor interactions between the potential antiviral peptides and the NEC. Here, the NEC was incubated with multilamellar vesicles (MLVs), with a known lipid composition for optimal NEC binding and budding (Bigalke et. al, 2014). MLVs were prepared at a 3:1:1 lipid ratio of POPC:POPS:POPA from 10 mg/mL stocks (in chloroform). Each lipid was suspended in combined in a glass vial and the solvent was evaporated under a light stream of argon gas while rotating to coat the vial with dried lipids. The MLVs were dried in a vacuum desiccator for 1 hour and rehydrated in gel filtration (GF) buffer.

Co-sedimentation (Pelleting) Assays

For NEC only controls, 3 µL NEC (17 µM) was incubated with 15 µL MLVs (10 mg/mL) GF buffer (50 µL total volume). For NEC with peptide studies, the same ratios were used as above but incorporated 10 µL peptide (at either 1 or 10 µM concentration). The components were combined in solution and incubated at room temperature for 30 minutes. After incubation of NEC, MLV, and peptide solutions, samples were centrifuged at 16,000xg and 4 °C for 20 minutes to pellet the liposomes out of solution. The supernatant was removed and separated from the pellet, and the pellet was resuspended in GF buffer.

For Tris/Tricine gels, samples were prepared by adding tricine sample buffer with β-mercaptoethanol (BME) and heating at 95 °C for 5 minutes. Both supernatant and pellet fractions were analyzed via gel electrophoresis using 16.5% Mini-PROTEAN® Tris/Tricine Precast Gels with the Precision Plus Protein™ Dual Xtra Prestained Protein Standard ladder. Gels were visualized using a BioRad ChemiDoc system.

For protein gels, samples were prepared by adding Laemmli sample buffer with BME, heated at 95 °C for 5 minutes, and analyzed by gel electrophoresis on 12% Mini-PROTEAN® TGX™ Precast Protein Gels using the PageRuler Plus Prestained Protein Ladder. Gel bands were visualized using a BioRad ChemiDoc system and quantified with ImageJ densitometry.

Percent density was calculated by dividing the intensity of the pellet or supernatant by the total intensity (pellet + supernatant) for each replicate. Replicates were averaged and graphed, with standard deviation represented as error bars.

Results

BLI identifies five peptides that interact with the NEC

Through biolayer interferometry (BLI), binding interactions between five designed peptides and the NEC were initially observed. The sequences of these peptides are displayed in Table 2. Selected peptides were short sequences taken from UL31 and UL34 at key points of NEC:NEC interactions (either hexameric or interhexameric). Figure 2 displays the 3D structure of the NEC, along with the side-views of three of the five identified peptides (Figure 2).

Original BLI screenings used a truncated construct of the NEC (NECΔ140-190) which does not contain regions of the NEC required for membrane interactions to assess potential NEC regions that bind to potential inhibitory peptides (Figure 3). Similar findings were obtained using the full-length NEC (NEC220; data not shown). Overall, these data suggest the designed peptides have interactions with the NEC, but it does not address specificity or how the interactions may occur.

Co-sedimentation assays quantify NEC/membrane binding

The NEC requires both proper membrane interactions and oligomerization into a hexameric lattice to undergo budding. Two assays are currently used to assess these properties: the co-sedimentation (pelleting) assay (Bigalke et al., 2014), which determines whether NEC binds to membranes, and the fluorescent giant unilamellar vesicle (GUV) budding assay (Thorsen et al., 2021), which assesses NEC ability to oligomerize and drive membrane deformation. Since NEC budding depends on both processes, disruptions in either membrane association or oligomerization could inhibit vesiculation.

To identify peptides that may interfere with NEC function, five peptides with an N-terminal 6-FAM tag (Figure 4) were first tested. This fluorescent label was included to enable

visualization in confocal budding assays; however, before proceeding with confocal imaging, it was necessary to confirm that the 6-FAM tag itself did not influence NEC behavior. To address this, a series of co-sedimentation assays were performed to determine whether the 6-FAM-tagged peptides affected NEC-membrane interactions or NEC heterodimer stability.

The pelleting assay distinguishes between two possible peptide effects:

1. **Blocking NEC-membrane interactions** – If a peptide prevents NEC from binding to membranes, NEC will remain in the supernatant rather than pelleting with the liposomes. This could occur if the peptide binds NEC and sterically inhibits its interaction with membranes, or if the peptide preferentially binds membranes and outcompetes NEC.
2. **Destabilizing NEC heterodimers** – If a peptide disrupts the UL31/UL34 complex, the components will separate, leading to UL31 and/or UL34 appearing in different fractions rather than pelleting together.

An initial pelleting assay was performed to assess NEC220 binding to membranes. In this assay, the sample is incubated with multilamellar vesicles (MLVs), followed by centrifugation to separate the pellet—containing membrane-bound sample—from the supernatant, which holds the unbound sample. Each sample was prepared twice as technical replicates for each biological replicate, and both fractions were analyzed using SDS-PAGE for visualization.

NEC220 is known to bind and bud 40% acidic liposomes (Bigalke et. al, 2014). To validate our experimental system, we performed this assay and confirmed that the NEC220 construct functioned as expected (Figure 5A). This was evident from the strong NEC signal in the pellet fraction when MLVs were present, compared to when MLVs were absent from the sample conditions. These results demonstrate that our assay system is consistent with previous reports.

Peptide 3-6-FAM exhibits disruption to NEC heterodimer stability

To assess for peptide perturbation of NEC membrane binding, we performed the same pelleting assay as above, but in the presence peptides, at varying NEC:peptide molar ratios. Peptide 1-6-FAM was first screened at a 1:1 NEC:peptide molar ratio (1X concentration), followed by a second assay at a 1:10 NEC:peptide molar ratio (10X concentration) to assess concentration-dependent effects. Both pellet and supernatant fractions were analyzed using 12% SDS-PAGE. As shown in Figure 5A, NEC remained in the pellet fraction in the presence of Peptide 1-6-FAM, indicating that the peptide does not disrupt NEC:membrane interactions. To further assess NEC and peptide behavior, this assay was repeated using Tris/Tricine peptide gels for improved resolution of NEC components UL31 and UL34 and the peptide. While faint bands corroborated the SDS-PAGE results (Figure 5B), NEC signals were often weak or indistinct (Figure 6). Subsequent Tris/Tricine assays failed to consistently detect NEC**,** leading to the decision to conduct all further assays using 12% SDS-PAGE gels.

Peptide 2-6-FAM was then tested under the same conditions as Peptide 1-6-FAM, with two technical replicates at 10X concentration. In the first assay, pellet bands were only visible in the NEC/MLV condition (Figure 7A, Figure 8). However, a second assay under identical conditions showed a strong pellet signal in the NEC-only control (Figure 7B). This inconsistency suggests experimental variability, such as pipetting errors or gel loading inconsistencies. Despite this, both assays demonstrated either no signal in the NEC/MLV/Peptide 2-6-FAM condition or a significant fraction of the NEC signal in the pellet, indicating that Peptide 2-6-FAM does not inhibit NEC/membrane interactions.

Peptide 3-6-FAM was evaluated by Tessa Larsen (BCDB Graduate Student), who conducted pelleting assays at 1X, 2X, and 10X NEC:peptide molar ratios. Across all conditions, NEC/membrane interactions remained unaffected, as indicated by the presence of NEC in the

pellet fraction (Figure 9). However, in the absence of MLVs, NEC heterodimer formation was disrupted, with UL31 shifting to the pellet and UL34 appearing in the supernatant (Figure 9). This effect was peptide concentration-dependent, with partial disruption at lower ratios and complete loss of the UL31 band at higher ratios (Figure 9B). These findings suggest that Peptide 3-6-FAM destabilizes the NEC heterodimer, though this disruption was overcome when NEC was bound to membranes.

Peptide 4-6-FAM was then tested using a 1:10 NEC:peptide molar ratio. A strong pellet signal was observed in the NEC-only control, while no signal was detected in the NEC/Peptide 4-6-FAM condition (Figure 10). These unexpected results were likely due to pipetting errors or a potential sample swap. A pelleting assay was not conducted for Peptide 5-6-FAM.

Effect of 6-FAM Tag Removal on NEC Binding

The untagged versions of Peptides 1–5 were tested to assess whether the removal of the 6-FAM tag affected NEC binding. Results confirmed that untagged Peptide 1 did not disrupt NEC/membrane interactions, consistent with prior findings (Figure 5, Figure 11). Similarly, untagged Peptide 2 showed no inhibitory effect, as evidenced by strong pellet signals in the NEC/MLV/Peptide 2 condition (Figure 12). For untagged Peptide 3, NEC heterodimer formation remained stable, with no disruption of UL31 or UL34 observed (Figure 13). The assay was repeated twice, yielding results identical to previous tests, suggesting that the FAM tag was likely responsible for the previously observed NEC heterodimer disruption (Figure 14). Untagged Peptide 4 also did not prevent NEC/MLV interactions, as indicated by strong pellet signals in the NEC/MLV/Peptide 4 condition (Figure 15). Peptide 5 was tested only in its untagged form. While it did not prevent NEC:MLV interactions, the pellet signal in the

NEC+MLV condition was unexpectedly reduced (Figure 16). This abnormality was attributed to experimental error.

Some Peptides Produced Changes to Sample pH

Throughout conducting the assays with the 6-FAM-tagged peptides, an unexpected color change was observed in Peptide 3-6-FAM solutions upon the addition of Laemmli sample buffer (Figure 17). This color shift, which indicated an acidic environment due to the yellowing of bromophenol blue, prompted further investigation into the pH of the solution. pH testing confirmed that Peptide 3-6-FAM solutions had a pH of 4.5, despite being prepared in a neutral buffer. We also observed that some of the non-FAM-tagged peptides exhibited similar behavior, with the addition of Laemmli buffer causing a color change. This suggested that the acidic pH could be destabilizing NEC, leading to the observed disruption of NEC heterodimer formation in Peptide 3-6-FAM assays (Figure 9).

Overall, the results suggest that non-FAM-tagged peptides generally do not prevent NEC/membrane interactions. This indicates that these peptides could be binding to NEC and inhibiting budding, but since the assay does not detect such interactions, we cannot visualize this effect in the pelleting assay. Therefore, while no disruption of NEC/membrane binding was observed, it is possible that these peptides are still modulating the NEC complex in a way that affects budding, just not in a manner detectable by this specific experimental approach.

Discussion

This study aimed to evaluate five peptides for their ability to inhibit NEC/membrane interactions. Using co-sedimentation assays, we tested whether these peptides prevented NEC association with membranes— an essential prerequisite for NEC lattice assembly and vesiculation. In these assays, NEC binding to membranes is indicated by the presence of NEC in the pellet fraction, while successful inhibition would result in NEC remaining in the supernatant. However, across all tested conditions, NEC was consistently detected in the pellet, regardless of peptide presence. This suggests that none of the peptides directly blocked NEC-membrane binding.

A key observation was that Peptide 3-6-FAM disrupted NEC heterodimer formation in the absence— but not presence— of membranes. This further supports the idea that membrane binding stabilizes the NEC complex, preventing dissociation even in the presence of destabilizing factors. Similar stabilization effects have been observed in previous HSV-1 NEC studies (Bigalke & Heldwein, 2016; Arii, 2021), where membrane-bound NEC complexes exhibited increased resistance to external perturbations. Initially, it was thought that this effect was specific to Peptide 3-6-FAM, but further investigation revealed that the acidity was likely due to trifluoroacetic acid (TFA) residue leftover from peptide lyophilization rather than the FAM tag itself. Some untagged peptides also exhibited pH-dependent behavior, reinforcing the idea that peptide preparation methods can introduce unintended chemical effects that alter NEC stability. Nevertheless, this validates an important notion in the field that NEC heterodimers are more flexible in the absence of membranes yet upon lattice formation, remain flexible enough to induce membrane curvature.

These findings emphasize an important consideration for future peptide-based NEC inhibitors: fluorescent tags, while useful for visualization, can introduce unwanted electrostatic

or pH-dependent effects. Additionally, peptide synthesis methods— particularly TFA-based lyophilization— should be carefully controlled, as residual acid can influence experimental outcomes. Future experiments should include rigorous peptide purification steps to minimize these confounding factors.

While this study demonstrates that the tested peptides do not disrupt NEC-membrane binding, this does not mean they lack inhibitory activity altogether. NEC inhibition may still occur by disrupting NEC oligomerization, thereby preventing lattice formation and vesiculation. Since this assay only measures membrane binding, it cannot determine whether NEC oligomerization is affected. Thus, while none of the peptides prevented NEC from associating with membranes, they may still interfere with later stages of NEC function, such as budding. To investigate this possibility, an alternative experimental approach, such as a confocal budding assay, is required.

The decision to begin with co-sedimentation assays rather than immediately conducting confocal budding assays was based on practical considerations. Confocal microscopy is costly and requires significant reagent consumption, making it inefficient for initial screening. The results from this study now provide a rationale for selecting specific peptides for follow-up testing in a confocal budding assay, allowing for a more targeted and efficient approach to identifying potential NEC inhibitors. Our lab is currently working to improve the confocal budding assay, using an alternative methodology and the peptides identified here will be a great use for this new method.

To further assess whether the peptides interfere with NEC oligomerization, future studies should incorporate chemical crosslinking experiments. Chemical crosslinking can stabilize NEC-NEC interactions, allowing for the detection of oligomeric species via SDS-PAGE or Western blotting. If peptides disrupt oligomerization, crosslinked NEC complexes would appear altered

compared to untreated controls. This approach would provide direct evidence for whether these peptides interfere with lattice formation, complementing the current findings.

Tables and Figures

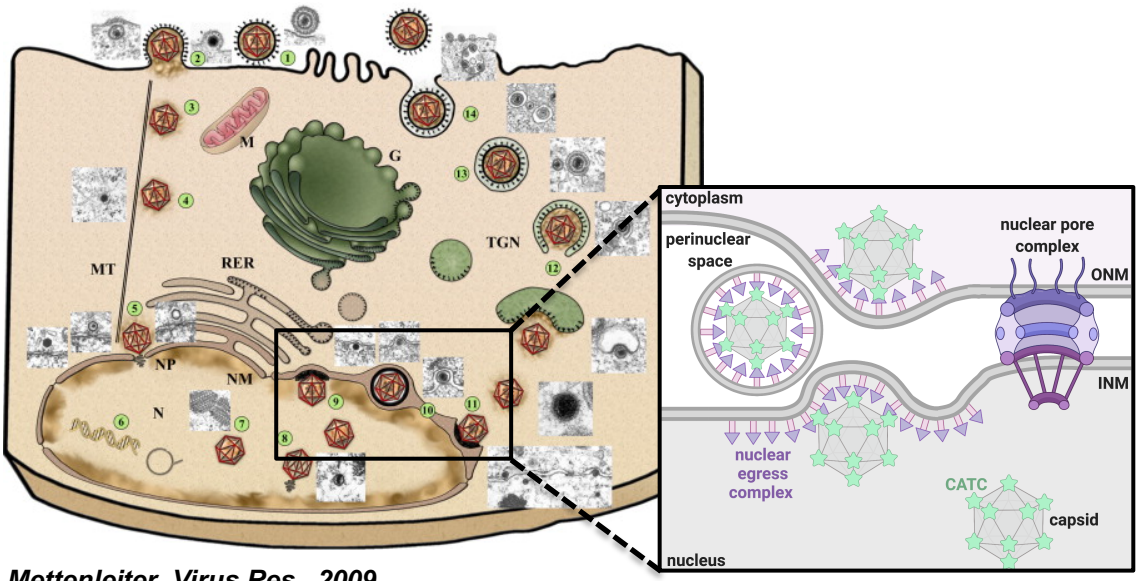

Mettenleiter, Virus Res., 2009

Draganova et al., Curr. Issues Mol. Biol., 2020

Figure 1. Mechanism of nuclear egress. Viral DNA is replicated in the host cell nucleus, and new viral proteins are produced. Newly formed capsids bud out of the nucleus at the inner nuclear membrane (INM), forming enveloped vesicles that fuse with the outer nuclear membrane, and release into the cytoplasm.

UL31 peptide position	Sequence	Binds to NEC?
27	NSLTLSGMGYYLGIG	Minimal
28	LSGMGYYLGIGGSSP	N
54	TSAHLH	N
55	TSAHLHYRLI	N
60	**ASPGYRFVAHVWQST**	**Y**
61	HVWQSTF	Minimal
63	QSTFVLVVRRNAEKP	N
64	VKTYYGMGGTGGSQ	N

UL34 peptide position	Sequence	Binds to NEC?
8	STLRGGDGEAGPYSP	N
9	GGDGEAGPYSPSSLP	Minimal
10	EAGPYSPSSLPSRSA	N
12	SLPSRSAFQFHGHDG	N
23	**NTGVSVLFQGFFHRP**	**Y**
28	GAITPERTNVILGST	N
29	PERTNVILGSTETTG	N
33	SLGDLDTIKGRLGLD	N
34	LDTIKGRLGLDARPM	N

Peptide Name	Sequence	Binds to NEC?
ED29	RETAAEQVVVLQAQR	N
ED30	AEQVVVLQAQRTAAA	N
ED31	VVLQAQRTAAAAALE	N
ED32	AAAAALENAAMAA	Minimal
ED23	RETAAEQVVVLQAQRTAA AAALENAAMAA	N

Table 1. Sequences of Peptides Derived from UL31 or UL34 Screened via BLI. A series of 15-amino acid peptides corresponding to hexameric or interhexameric interfaces within UL31 or UL34 were screened for NEC binding using biolayer interferometry (BLI). This high-throughput assay measures binding interactions based on changes in refractive index within individual biosensors. Of the peptides tested, two demonstrated binding to the NEC construct NECΔ40-190.

Peptide	Sequence	Protein	Residues
Peptide 1	NTGVSVLFQGFFHRP	UL34	89-103
Peptide 2	NSLTLSGMGYYLGIG	UL31	105-119
Peptide 3	**ASPGYRFVAHVWQST**	**UL31**	**237-251**
Peptide 4	HVWQST	UL31	246-251
Peptide 5	GTSAHLHYRLIDRML	UL31	221-235

Table 2. Potential inhibitory peptides and protein origins. Five distinct peptides were identified through BLI screening as exhibiting binding with NEC220.

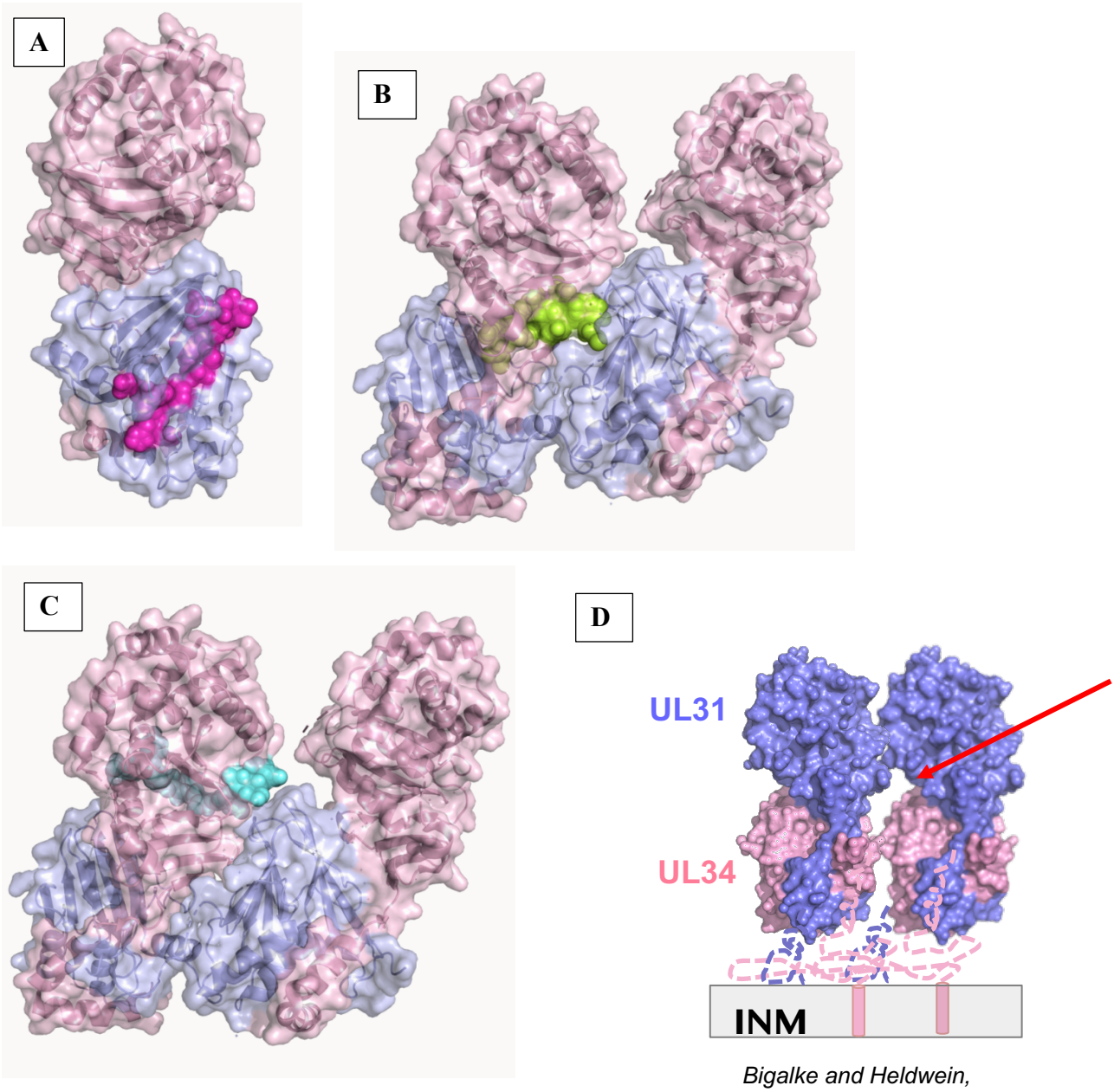

Figure 2. 3D structure of the NEC and side views of three identified membrane-interacting peptides. (A–C) Structural representations of Peptide 1, Peptide 2, and Peptide 3, highlighting their conformations and potential interaction surfaces. (D) The 3D structure of the NEC, showing the UL31 and UL34 subunits interacting with each other and associating with the inner nuclear membrane. This visualization provides insight into how these peptides may interact with the NEC or membrane to modulate NEC activity.

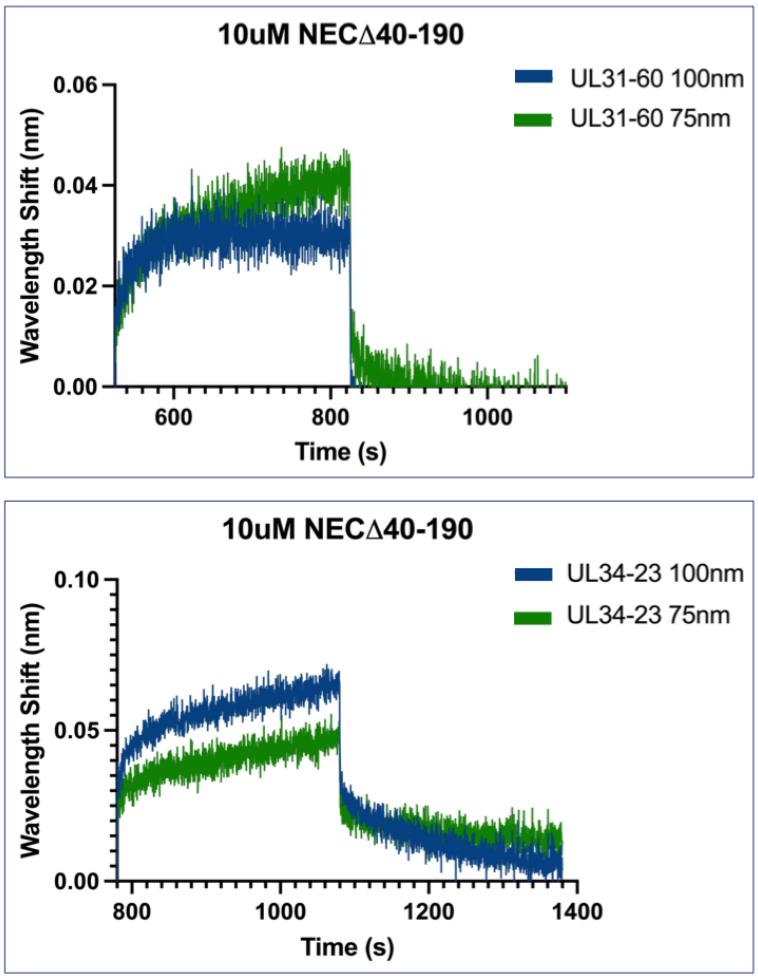

Figure 3. Example BLI screening conducted on truncated construct NECΔ140-190. Screening tested the binding affinity of two peptides, UL31-60 and UL34-23. In this BLI assay, binding is detected by an increase in optical density (response units) as the NEC interacts with biotinylated peptides immobilized on streptavidin-coated biosensors. A positive binding result is characterized by a distinct upward shift in response units upon peptide association, followed by a gradual decrease (dissociation phase) when the peptide is removed. Stronger binding interactions result in a higher response and slower dissociation, while weak or no binding produces minimal changes.

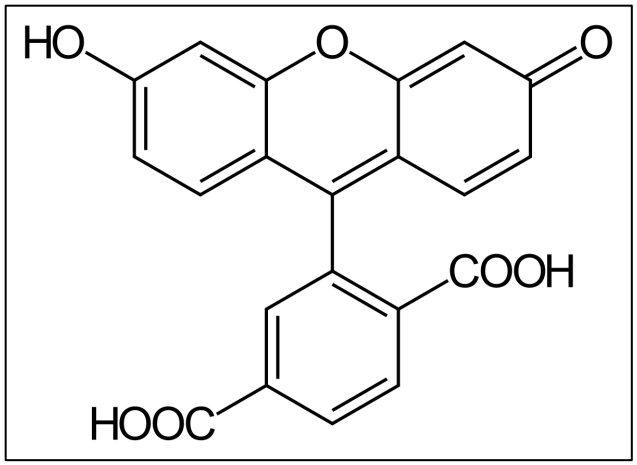

Figure 4. Structure of 6-FAM tag. Peptides were purchased with the addition of the 6-FAM tag to ensure visualization of peptide localization with respect to the NEC would be possible during confocal budding assays.

Figure 5A. 1X, 10X Concentrations, 12% SDS PAGE, Peptide 1-6-FAM

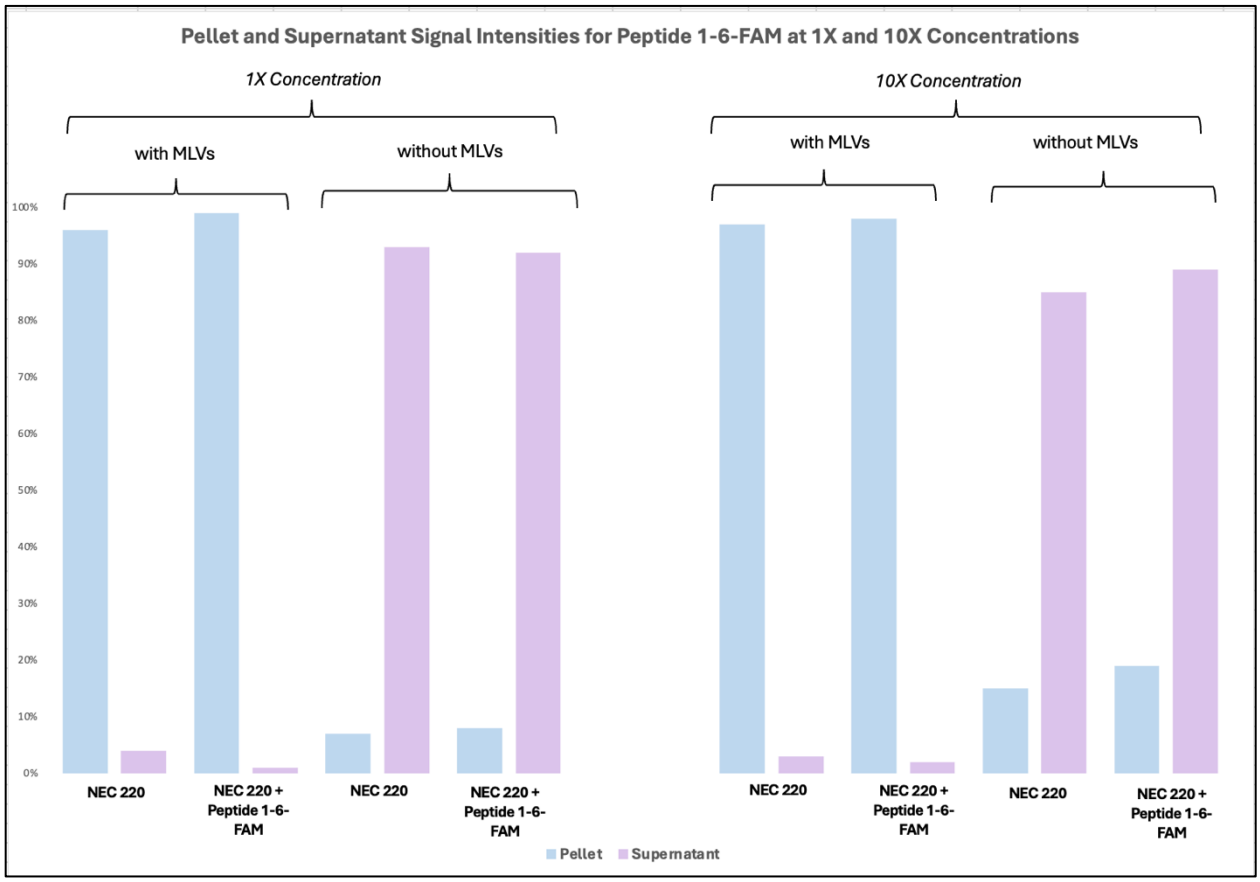

Figure 5B. 10X Concentrations, Tris/Tricine, Peptide 1-6-FAM

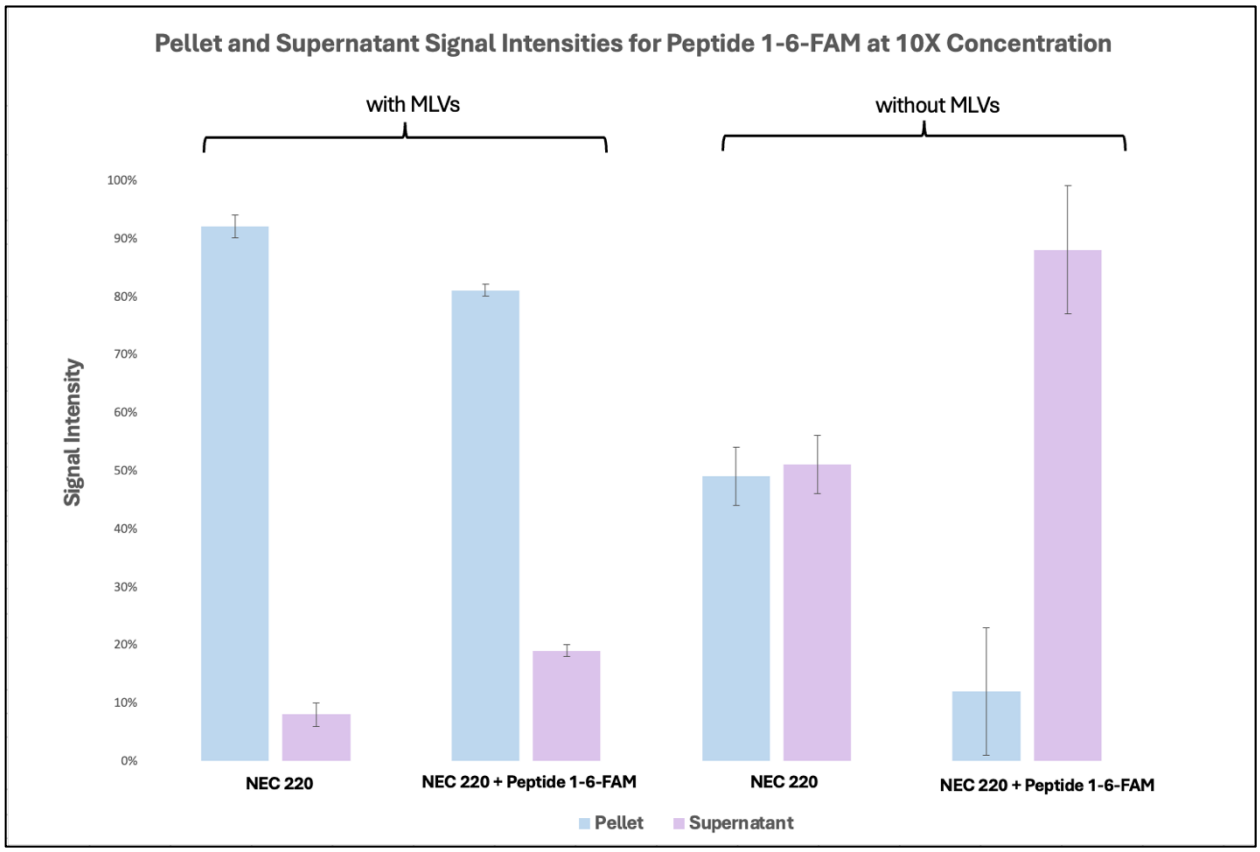

Figure 5. Quantification of pellet signal intensity for NEC 220 and Peptide 1-6-FAM across different experimental conditions. (A) Signal intensity of the pellet fraction analyzed using a 12% SDS-PAGE gel for various conditions involving NEC 220 alone, NEC 220 with multilamellar vesicles (MLVs), and NEC 220 with Peptide 1 in the presence or absence of MLVs. Bars represent mean signal intensity, with error bars indicating standard deviation. Different concentrations (1X and 10X) were tested for NEC 220 and Peptide 1-6-FAM conditions. (B) Signal intensity of the pellet fraction analyzed using a Tris/Tricine gel, comparing conditions: NEC 220 with MLVs, NEC 220 alone, NEC 220 with Peptide 1-6-FAM and MLVs, and NEC 220 with Peptide 1-6-FAM only. Bars represent mean signal intensity, with error bars indicating standard deviation. Bars marked with asterisks denote a lack of signal in the gel lane corresponding to the sample condition.

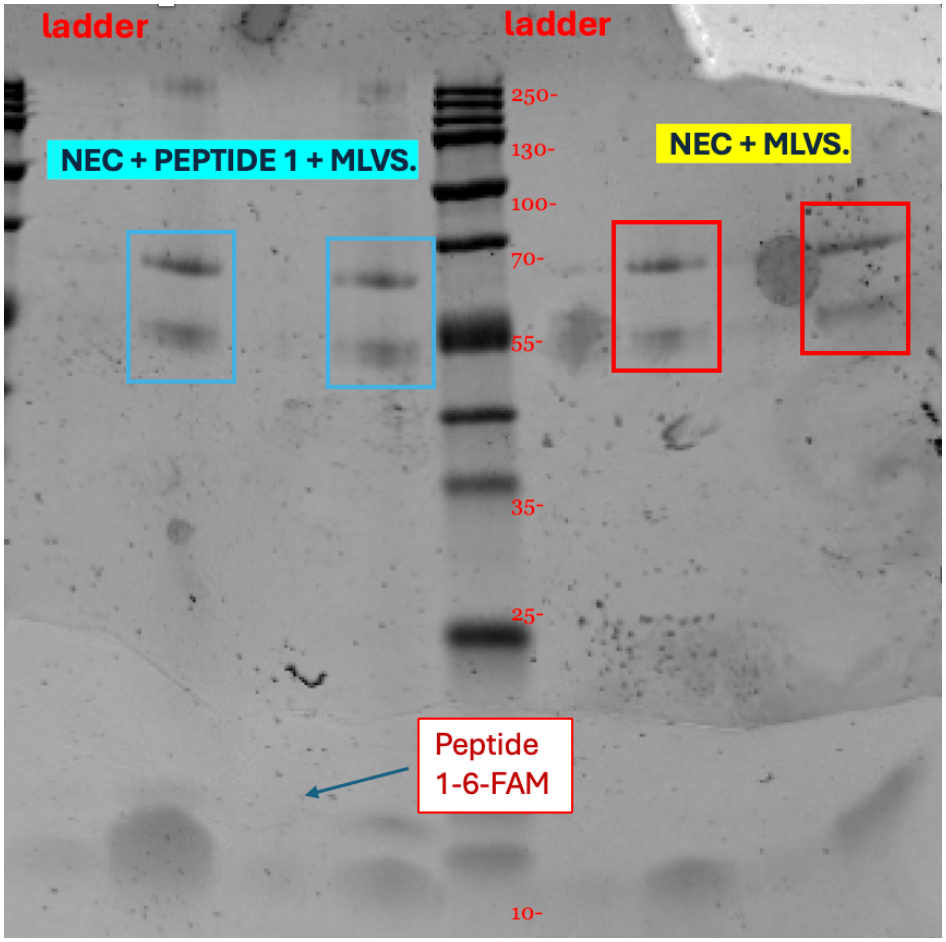

Figure 6. Peptide 1-6-FAM assays run on Tris/Tricine gels. This gel displays the NEC, Peptide 1-6-FAM, and MLV condition, as well as the NEC and MLV condition of the assay. NEC signals are weak and indistinct. Peptide 1-6-FAM is visible at the bottom of the gel.

Figure 7A. 10X Concentration, Peptide 2-6-FAM, Assay 1

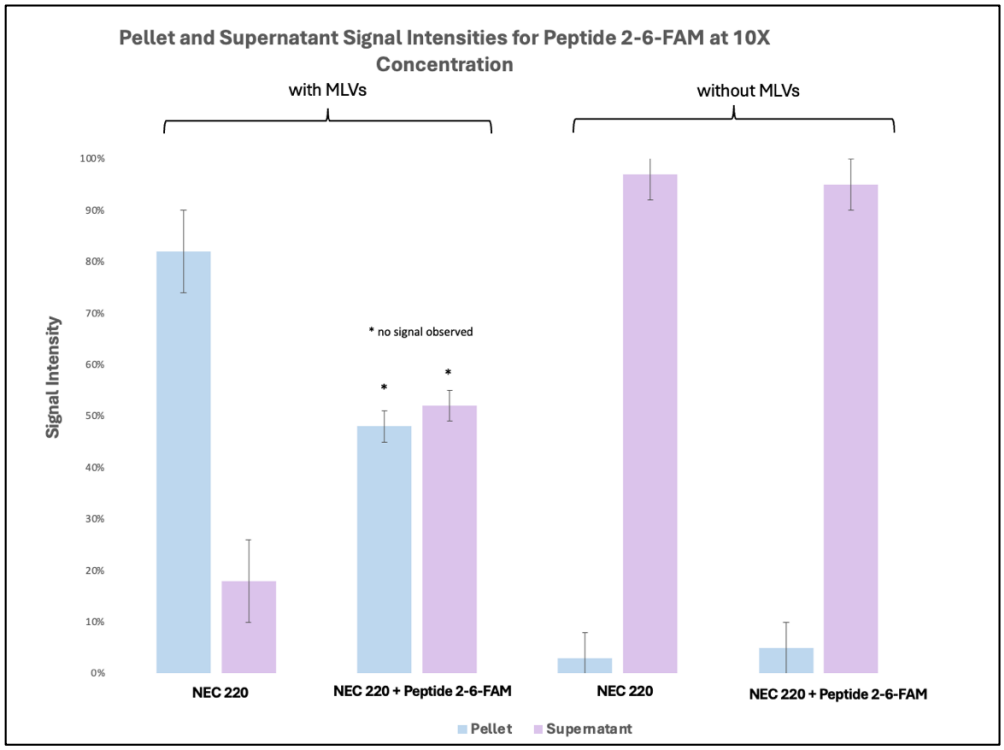

Figure 7B. 10X Concentration, Peptide 2-6-FAM, Assay 2

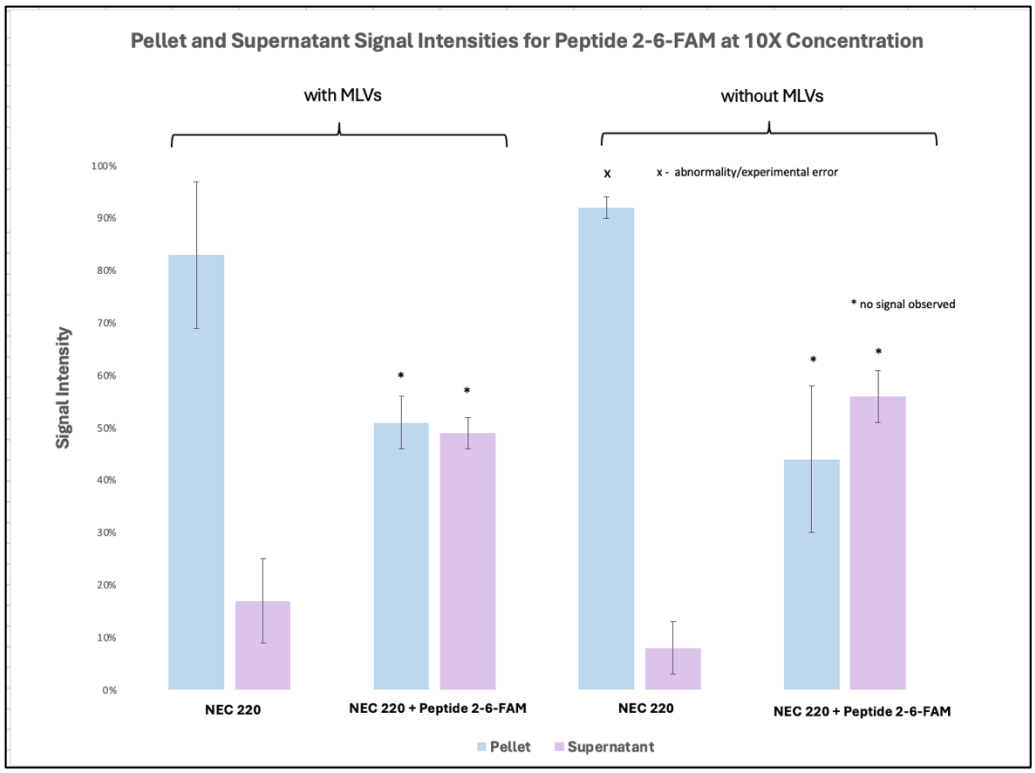

Figure 7. Pellet and Supernatant Signal Intensities for Peptide 2-6-FAM at 10X Concentration. Signal intensity of the pellet fraction analyzed using a 12% SDS-PAGE gel,

comparing NEC 220 alone, NEC 220 with multilamellar vesicles (MLVs), and NEC 220 with Peptide 2 containing the 6-FAM tag in the presence or absence of MLVs. Peptide 2 was used at a 1:10 NEC:peptide molar ratio (10X concentration), with two experimental replicates. 5A + 5B denote two experiments performed using peptide 2-6-FAM, both performed under the same conditions. Bars represent mean signal intensity, with error bars indicating standard deviation. Bars marked with asterisks denote a lack of signal in the gel lane corresponding to the sample condition.

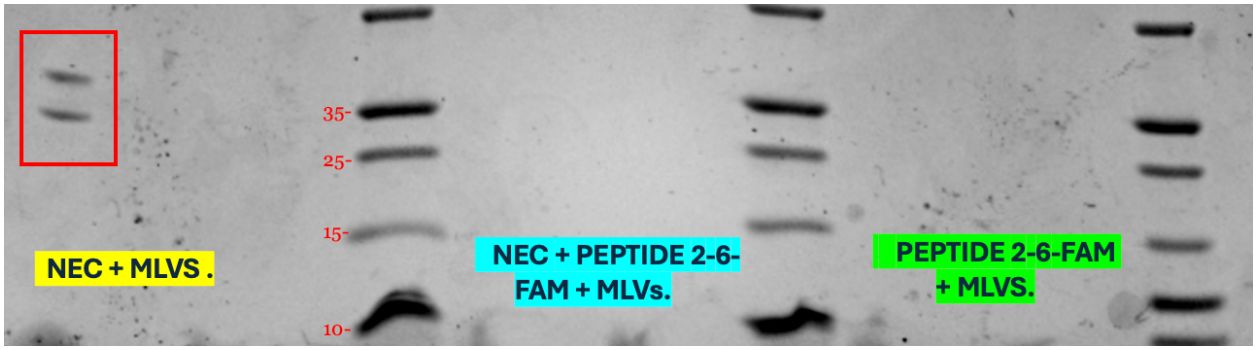

Figure 8. Initial assay conducted with peptide 2-6-FAM. Pellet signal only visible in the NEC with MLVs condition. No signal appears in the NEC, peptide 2-6-FAM, and MLVs condition or the peptide 2-6-FAM with MLVs condition.

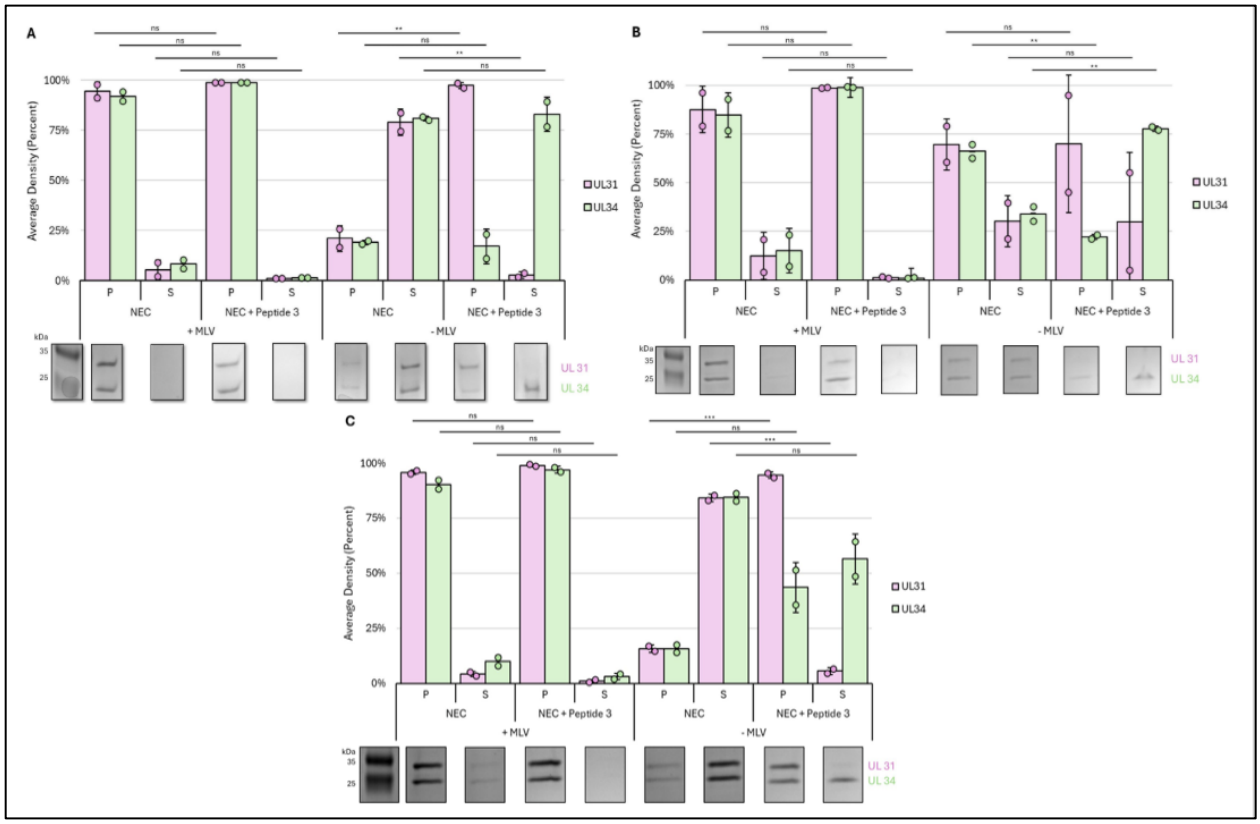

Figure 9. Peptide 3-6-FAM assessed at 1X, 2X, and 10X concentrations. Each graph displays

signal intensity of the pellet fraction analyzed using a 12% SDS-PAGE gel, comparing NEC 220 alone, NEC 220 with multilamellar vesicles (MLVs), and NEC 220 with Peptide 3 containing the 6-FAM tag in the presence or absence of MLVs. Each assay was done in two technical replicates. (A) Pelleting assay assessed at a 2X peptide 3-6-FAM concentrations. NEC heterodimer is disrupted in presence of peptide 3-6-FAM and absence of MLV. UL31 crashes out of solution. (B) Pelleting assay assessed at a 10X peptide 3-6-FAM concentrations. NEC heterodimer is disrupted and UL31 is lost. (C) Pelleting assay assessed at a 1X peptide 3-6-FAM concentrations. NEC heterodimer is disrupted and UL31 and some UL34 crash out. Error bars at the top of each graph represent statistical significance. Graph generated by Tessa Larsen (BCDB Graduate Student).

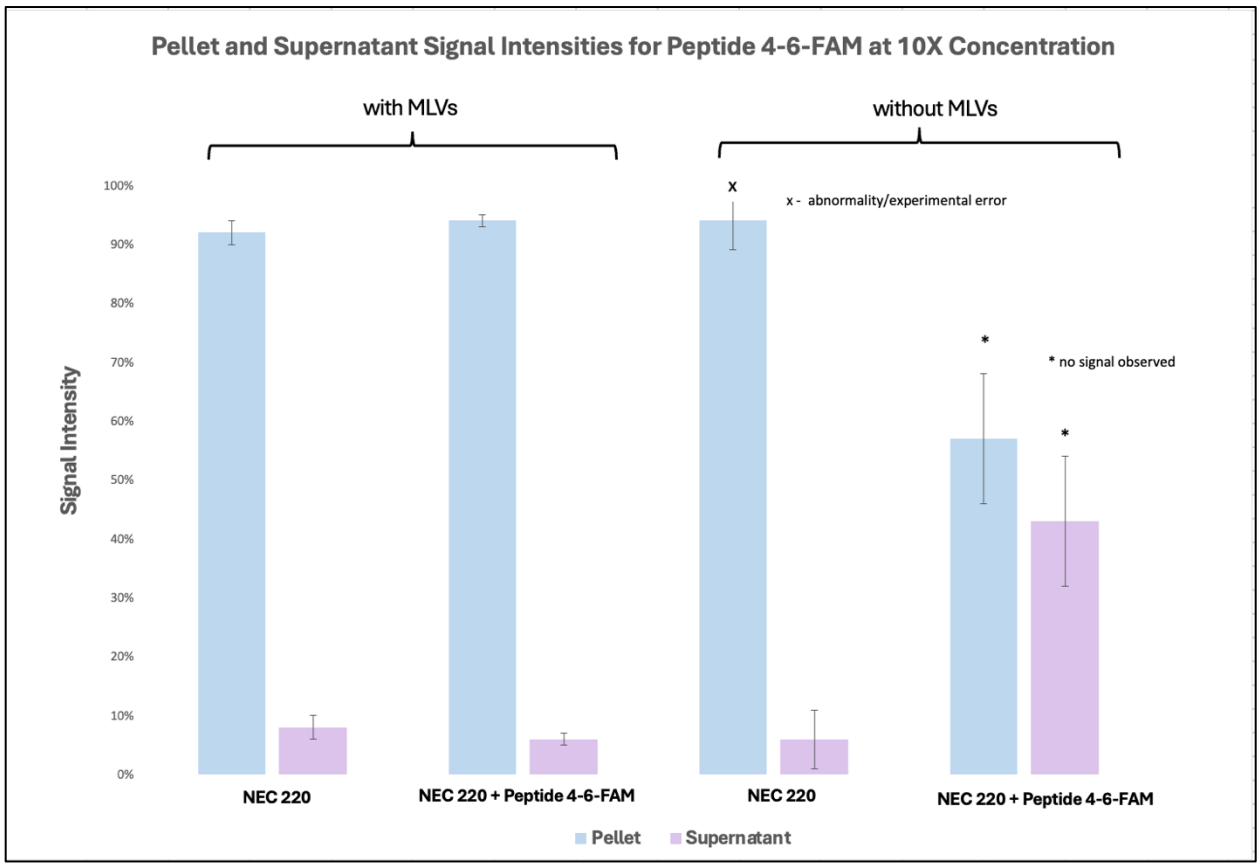

Figure 10. Pellet and Supernatant Signal Intensities for Peptide 4-6-FAM at 10X Concentration. Signal intensity of the pellet fraction analyzed using a 12% SDS-PAGE gel, comparing NEC 220 alone, NEC 220 with multilamellar vesicles (MLVs), and NEC 220 with Peptide 4 containing the 6-FAM tag in the presence or absence of MLVs. Peptide 4 was used at a 1:10 NEC:peptide molar ratio (10X concentration), with two experimental replicates. Bars marked with asterisks denote a lack of signal in the gel lane corresponding to the sample

condition. Bars marked with ‘x’ denote the presence of an abnormality/ potential experimental error.

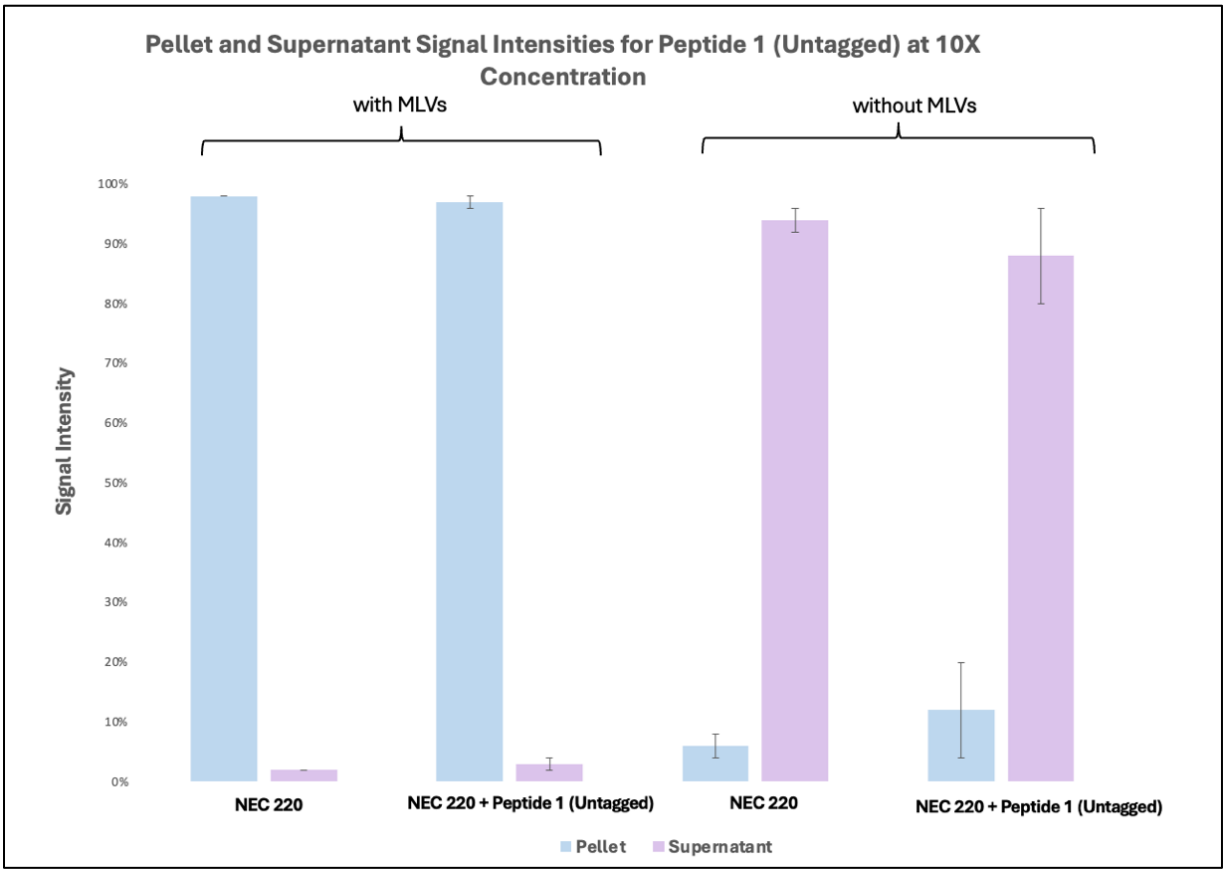

Figure 11. Pellet and Supernatant Signal Intensities for Peptide 1 (Untagged) at 10X Concentration. Signal intensity of the pellet fraction analyzed using a 12% SDS-PAGE gel, comparing NEC 220 alone, NEC 220 with multilamellar vesicles (MLVs), and NEC 220 with Peptide 1 (without the FAM tag) in the presence or absence of MLVs. Peptide 1 was used at a 1:10 NEC:peptide molar ratio (10X concentration), with two experimental replicates. Bars represent mean signal intensity, with error bars indicating standard deviation.

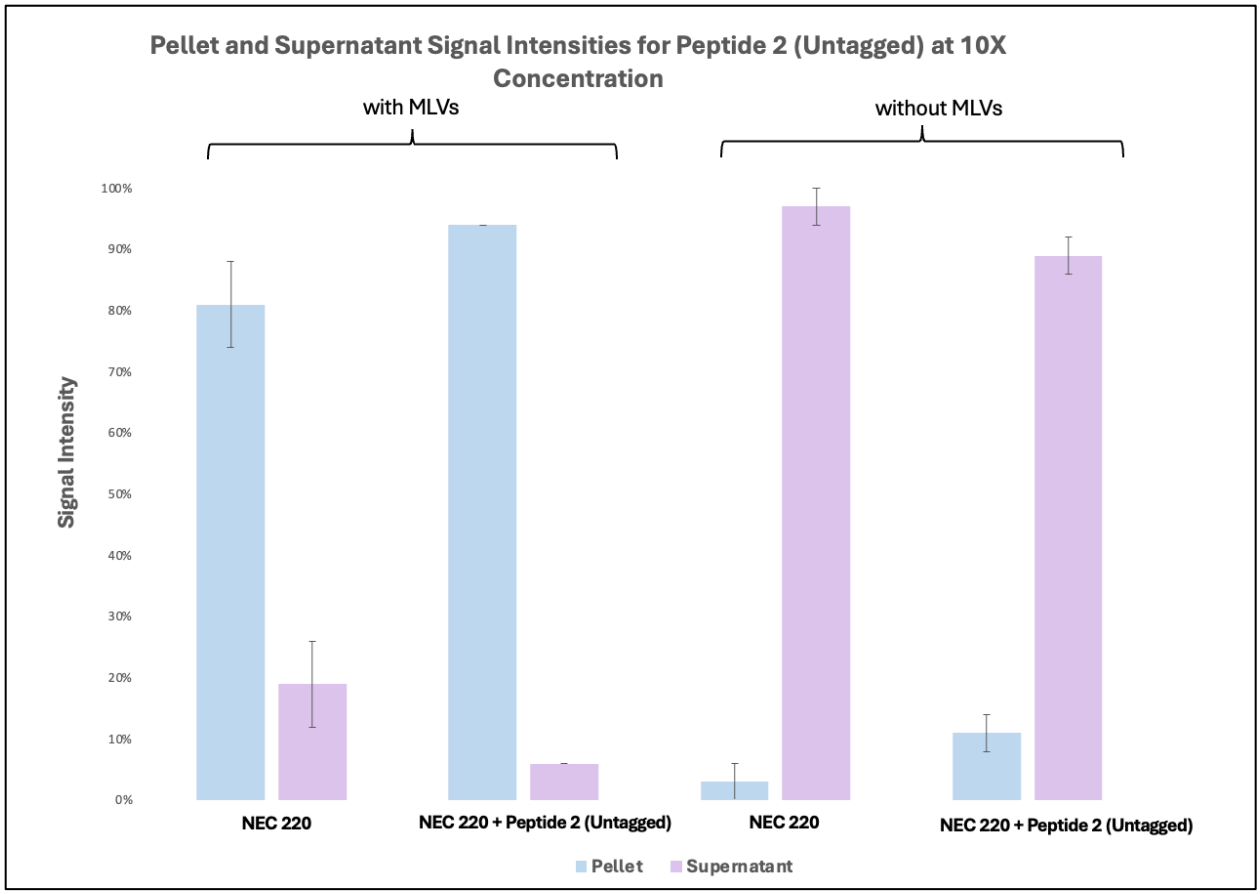

Figure 12. Pellet and Supernatant Signal Intensities for Peptide 2 (Untagged) at 10X Concentration. Signal intensity of the pellet fraction analyzed using a 12% SDS-PAGE gel, comparing NEC 220 alone, NEC 220 with MLVs, and NEC 220 with Peptide 2 lacking the 6-FAM tag in the presence or absence of MLVs. Peptide 2 was used at a 1:10 NEC:peptide molar ratio (10X concentration), with two experimental replicates. Bars represent mean signal intensity, with error bars indicating standard deviation.

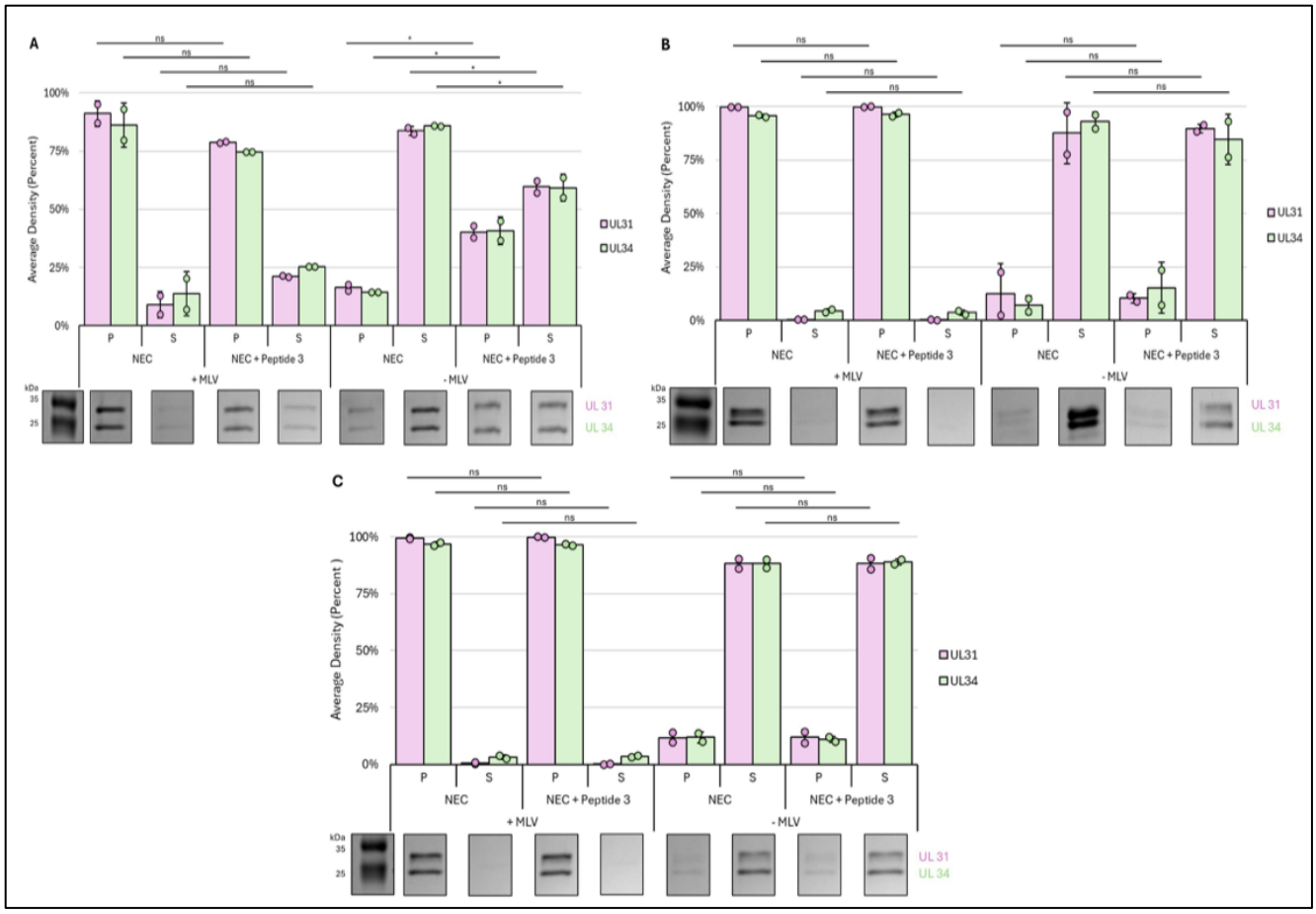

Figure 13. Peptide 3 (untagged) assessed at 1X, 2X, and 10X concentrations. Each graph displays signal intensity of the pellet fraction analyzed using a 12% SDS-PAGE gel, comparing NEC 220 alone, NEC 220 with multilamellar vesicles (MLVs), and NEC 220 with Peptide 3 (untagged) in the presence or absence of MLVs. Untagged peptide 3 inconsistently destabilizes NEC heterodimer in the absence of MLV. Each assay was done in two technical replicates, and symbols represent each replicate. (A) Pelleting assay assessed at 1X peptide 3 concentrations. Some NEC crashes out of solution in the presence of peptide 3 and absence of MLV. (B-C) Pelleting assays assessed at 1X (B) and 10X (C) peptide 3 concentrations. Peptide 3 has no significant impact on NEC heterodimer formation. Error bars at the top of each graph represent statistical significance. Graph generated by Tessa Larsen (BCDB Graduate Student).

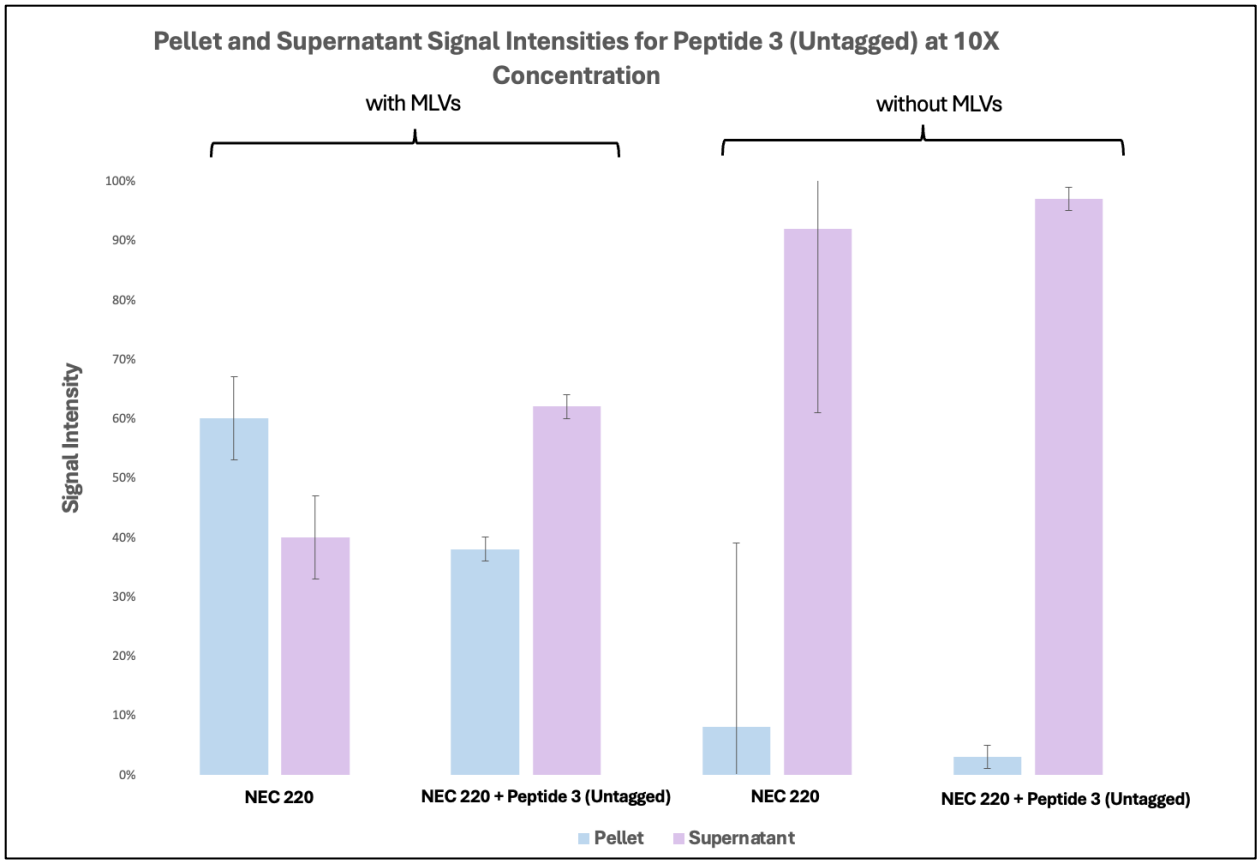

Figure 14. Pellet and Supernatant Signal Intensities for Peptide 3 (Untagged) at 10X Concentration. Signal intensity of the pellet fraction analyzed using a 12% SDS-PAGE gel, comparing NEC 220 alone, NEC 220 with MLVs, and NEC 220 with Peptide 3 lacking the 6-FAM tag in the presence or absence of MLVs. Peptide 3 was used at a 1:10 NEC:peptide molar ratio (10X concentration), with two experimental replicates. Bars represent mean signal intensity, with error bars indicating standard deviation.

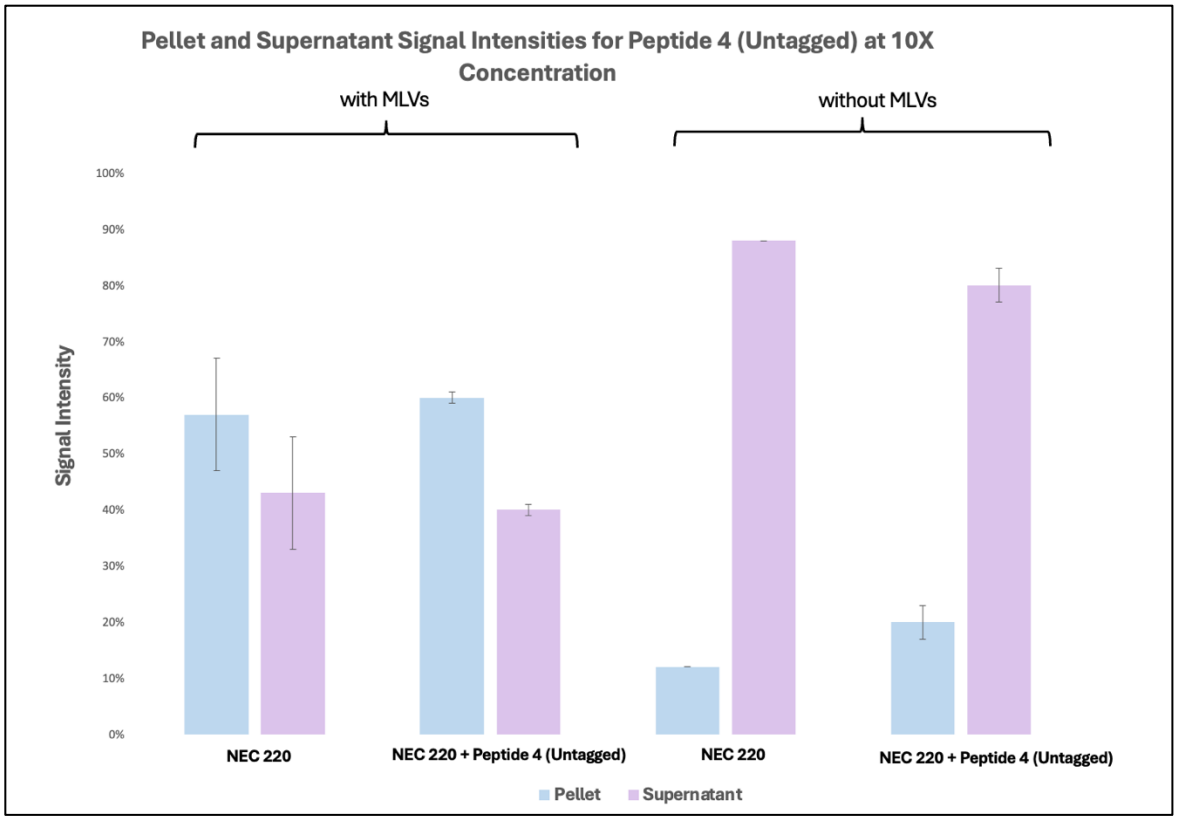

Figure 15. Pellet and Supernatant Signal Intensities for Peptide 4 (Untagged) at 10X Concentration. Signal intensity of the pellet fraction analyzed using a 12% SDS-PAGE gel, comparing NEC 220 alone, NEC 220 with MLVs, and NEC 220 with Peptide 4 lacking the 6-FAM tag in the presence or absence of MLVs. Peptide 4 was used at a 1:10 NEC:peptide molar ratio (10X concentration), with two experimental replicates. Bars represent mean signal intensity, with error bars indicating standard deviation.

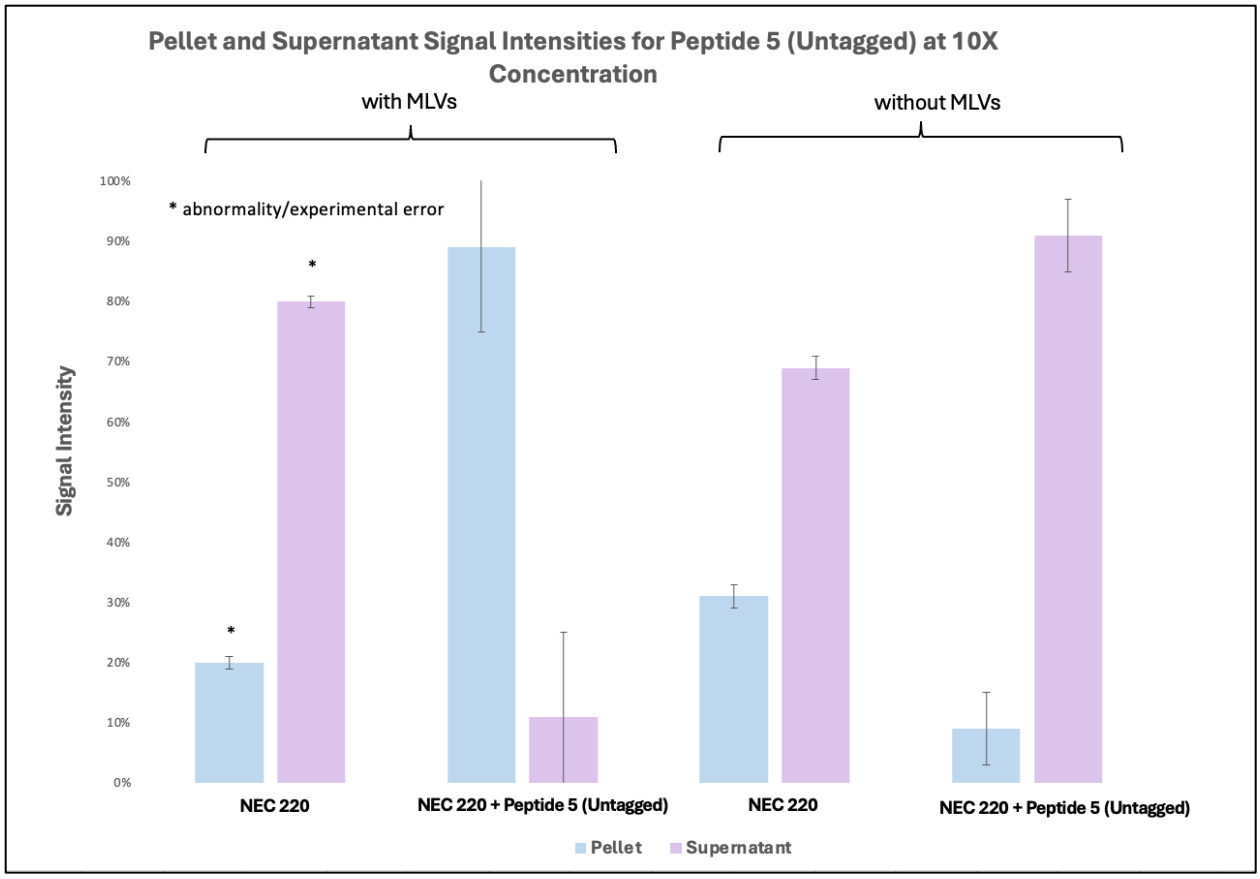

Figure 16. Quantification of pellet signal intensity for NEC 220 with Peptide 5 lacking the 6-FAM tag. Signal intensity of the pellet fraction analyzed using a 12% SDS-PAGE gel, comparing NEC 220 alone, NEC 220 with multilamellar vesicles (MLVs), and NEC 220 with Peptide 5 lacking the 6-FAM tag in the presence or absence of MLVs. Peptide 5 was used at a 1:10 NEC:peptide molar ratio (10X concentration), with two experimental replicates. Bars represent mean signal intensity, with error bars indicating standard deviation.

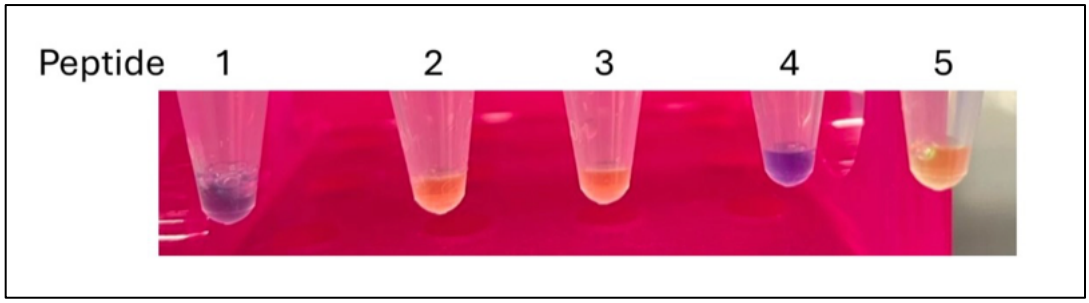

Figure 17. Peptides 1-5 6-FAM in solution with Laemmli buffer. Peptides 2, 3, and 5 turned yellow upon addition of sample buffer, indicating acid pH.

References

1. Arii, J. (2021). Host and viral factors involved in nuclear egress of Herpes Simplex Virus 1. *Viruses*, 13(5), 754. https://doi.org/10.3390/v13050754
2. Bigalke, J. M., & Heldwein, E. E. (2016). Nuclear exodus: Herpesviruses lead the way. *Annual Review of Virology*, 3(1), 387–409. https://doi.org/10.1146/annurev-virology-110615-042215
3. Bigalke, J. M., et al. (2014). Membrane deformation and scission by the HSV-1 nuclear egress complex. *Nature Communications*, 5(1). https://doi.org/10.1038/ncomms5131
4. Boehmer, P., & Nimonkar, A. (2003). Herpes virus replication. *IUBMB Life*, 55(1), 13–22. https://doi.org/10.1080/1521654031000070645
5. Bjerke, S. L., et al. (2003). The U(L)31 and U(L)34 gene products of herpes simplex virus type 1 are required for egress of capsids from the nucleus, but not for targeting of capsids to the intranuclear membrane. *Journal of Virology*, 77(17), 9733-9743.
6. Bradshaw, M. J., & Venkatesan, A. (2016). Herpes simplex virus-1 encephalitis in adults: Pathophysiology, diagnosis, and management. *Neurotherapeutics*, 13(3), 493–508.
7. Chen, H., et al. (2023). A small molecule exerts selective antiviral activity by targeting the human cytomegalovirus nuclear egress complex. *PLOS Pathogens*, 19(11). https://doi.org/10.1371/journal.ppat.1011781
8. Draganova, E. B., Zhang, J., Zhou, Z. H., & Heldwein, E. E. (2020). Structural basis for capsid recruitment and coat formation during HSV-1 nuclear egress. *Elife*, 9. https://doi.org/10.7554/eLife.56627
9. Draganova, E. B., et al. (2021). The ins and outs of herpesviral capsids: Divergent structures and assembly mechanisms across the three subfamilies. *Viruses*, 13(10), 1913. https://doi.org/10.3390/v13101913
10. Draganova, E. B., Wang, H., et al. (2024). The universal suppressor mutation restores membrane budding defects in the HSV-1 nuclear egress complex by stabilizing the oligomeric lattice. *PLOS Pathogens*, 20(1). https://doi.org/10.1371/journal.ppat.1011936
11. Fatahzadeh, M., & Schwartz, R. A. (2007). Human herpes simplex virus infections: Epidemiology, pathogenesis, symptomatology, diagnosis, and management. *Journal of the American Academy of Dermatology*, 57(5), 737-763.

12. Fuchs, W., et al. (2002). The UL31 gene product of pseudorabies virus is involved in secondary envelopment of virions and egress from the nucleus. *Journal of Virology*, 76(8), 364–378.
13. Itzhaki, R. F. (2018). Corroboration of a major role for herpes simplex virus type 1 in Alzheimer's disease. *Frontiers in Aging Neuroscience*, 10. https://doi.org/10.3389/fnagi.2018.00324
14. Johnston, C., et al. (2014). Current status and prospects for development of a vaccine against herpes simplex virus infections. *Vaccine*, 32(14), 1553-1560.
15. Klupp, B. G., et al. (2007). Pseudorabies virus UL31, a protein with weak sequence similarity to herpes simplex virus type 1 UL31, functions in capsid egress from the nucleus. *Journal of Virology*, 81(2), 767-777.
16. Miranda-Saksena, M., Denes, C. E., Diefenbach, R. J., & Cunningham, A. L. (2018). Infection and transport of Herpes Simplex Virus Type 1 in neurons: Role of the cytoskeleton. *Viruses, 10*(2), 92. https://doi.org/10.3390/v10020092
17. Otth, C. (2016). Herpes simplex virus type 1 at the central nervous system. *IntechOpen.* https://doi.org/10.5772/64198
18. Roller, R. J., & Baines, J. D. (2017). Herpesvirus nuclear egress. *Journal of Virology*, 91(2). https://doi.org/10.1128/JVI.01548-21
19. Roller, R. J., et al. (2010). Analysis of a charge cluster mutation of herpes simplex virus type 1 UL34 and its extragenic suppressor suggests a novel interaction between pUL34 and pUL31 that is necessary for membrane curvature around capsids. *Journal of Virology*, 84(8), 3921–3934. https://doi.org/10.1128/jvi.01638-09
20. Thorsen, M. K., et al. (2021). Highly basic clusters in the herpes simplex virus 1 nuclear egress complex drive membrane budding by inducing lipid ordering. *mBio*, 12(4). https://doi.org/10.1128/mbio.01548-21
21. Whitley, R. J., & Roizman, B. (2001). Herpes simplex viruses. *Virology*, 66, 123-164.